The Intimate Connection between High and Low Frequency Emission in Blazars

Alan P. Marscher [*]

Institute for Astrophysical Research, Boston University, 725 Commonwealth Ave., Boston,
MA 02215, USA

Abstract The author discusses the relationship between X and γ radiation and radio to optical emission in blazars based on recent observations. The availability of densely-sampled light curves at several wavebands for several quasars, BL Lacertae, and two radio galaxies demonstrates that a strong connection exists between high and low frequency emission. The relativistic jet provides the most straightforward explanation of this connection. In the radio galaxies, temporary decreases in the X-ray flux from the central engine precede the appearance of bright superluminal knots in the radio jet. The combination of multiwaveband light curves and millimeter-wave imaging with very long baseline interferometry, along with polarization measurements whenever possible, can map the emission regions and lead to more accurate theoretical descriptions of the physical processes in blazars than has been possible in the past.

Key words: active — galaxies: quasars: individual (3C 279, PKS 1510−089) galaxies: individual (3C 111, 3C 120) — galaxies: jet

1 INTRODUCTION

Although there has been justifiably great interest in γ-ray bursts recently, active galactic nuclei (AGN) remain the most energetic long-lived phenomena in the universe. Blazars are the most extreme type of AGN, emitting highly variable, nonthermal radiation across the electromagnetic spectrum. Although the power of all AGNs derives from the central engine, thought by most to be an accreting supermassive black hole, the spectral energy distribution (SED) is dominated by emission from a relativistic jet pointing almost directly into our line of sight. The jets consist of ultra-high energy particles imbedded in magnetic fields, with the entire plasma flowing outward from the nucleus at speeds that can extremely close to the speed of light, with corresponding bulk Lorentz factors that can exceed 40 (Jorstad et al. 2005). This creates two observational illusions: apparent superluminal motion of bright spots in very long baseline interferometric (VLBI) images, and time compression of variations in flux and polarization.

Decades after discovering relativistic jets, we are still struggling to figure out how nature manages to accelerate and collimate the flow, as well as energize the particles, with such high efficiency. The prevalent current thought among theorists is that the jet is launched by the twisting magnetic field of either the inner accretion disk or the ergosphere of the black hole, or even both (see Meier, Koide & Uchida 2000 for a review). If both the disk and ergosphere do the job, then the jets of blazars might contain a (relatively) slow spine-fast sheath structure. Population statistics show that Doppler favoritism in flux-limited samples is very strong, so fast spines with Lorentz factors $\Gamma > 5$ are very rare per unit cosmic volume (Lister & Marscher 1997). Either nature suppresses the emission of radiation in most of the spines or, more likely, the ultrafast motions seen in many blazars (Jorstad et al. 2001a, 2005) indicate that these objects possess the most highly relativistic jets of all the AGN that have fluxes high enough to appear in flux-limited surveys.

---

[*] E-mail: marscher@bu.edu
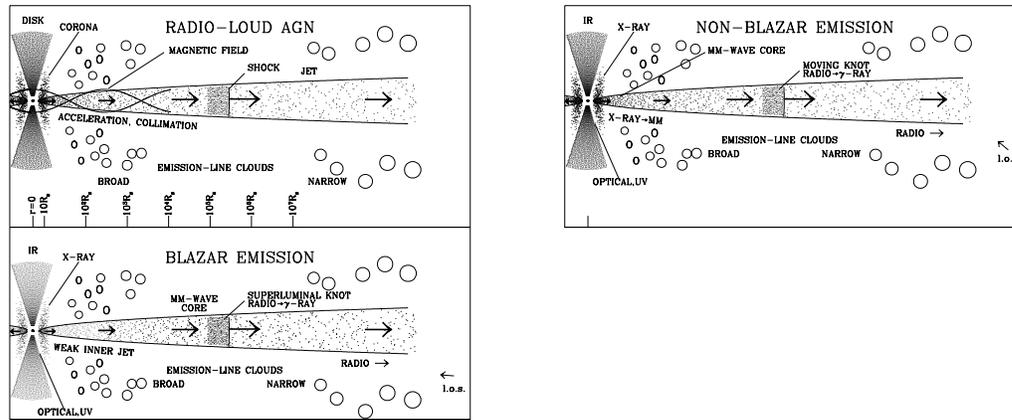
Fig. 1 Rough sketch of the structure and emission regions of a radio-loud active galaxy with a relativistic jet. Note the logarithmic scale on the bottom for the distance down the jet. In the two emission panels—one for jets viewed almost end-on (a blazar) and the other for those seen at a wider angle (a typical radio galaxy)—the likely waveband of photons that can be emitted at each site is indicated. If the jet accelerates out to parsec scales, the inner jet between the mm-wave core and the black hole may be essentially invisible in blazars, while in radio galaxies bright emission might extend down to the base of the jet. (Adapted from Marscher 2005.)

Intensive studies of blazars are therefore probing the most extreme physical ramifications of an accreting supermassive black hole. Blazars are also fun to follow as their SEDs rise, fall, and shift on amazingly rapid timescales.

The strong Doppler beaming causes the emission from blazars to dominate over that of the unbeamed radiation that stands out in the more mundane active galaxies (see Fig. 1). Of course, much can be learned by studying jets viewed side-on and from those observed in X-ray binaries, but only blazars allow us to taste all the flavors from the menu offered by highly relativistic jets.

What follows is a summary of the intensive multiwaveband monitoring program of several blazars and two radio galaxies that act as blazars at radio wavelengths, being carried out by the author and collaborators. This is an update of earlier preliminary results presented in Marscher et al. (2004).

2 THEORETICALLY EXPECTED CORRELATION OF LIGHT CURVES

The prevailing theory of emission from blazars holds that the radio to optical (and sometimes higher-frequency) portion of the SED corresponds to beamed synchrotron radiation from the jet. Except for objects whose SED peaks at X-ray energies, the primary X-ray production mechanism is synchrotron self-Compton (SSC) scattering. At GeV γ-ray energies, the emission is also inverse Compton, but could be either scattering of synchrotron photons in the jet or of ambient photons from emission-line clouds, a dusty torus, or some other source external to the jet. In the case of SSC, the X-ray variability should either be simultaneous with, or lag slightly, the lower-freqency fluctuations, i.e., there should be a correlation across wavebands with frequency-dependent time delays. (Sokolov, Marscher & McHardy 2004).

The correlation might be only modest, however, if there are gradients in the highest electron energies. This is expected if either the energization of electrons is restricted to particular locations, e.g., at shock fronts (Marscher & Gear 1985), or the efficiency of particle acceleration varies from one place to another in the jet. In the former case, rapid radiative cooling of the highest-energy electrons restricts the highest-frequency synchrotron emission to regions very close to where the energization occurs. The longer-lived lower-energy electrons can spread across a larger volume. If the particle acceleration produces a power-law

energy distribution (as opposed, for example, to a mono-energetic distribution whose energy changes with time), when a fresh region of energization (e.g., a new shock) arises, a flare will start at all optically thin frequencies simultaneously, but will peak earlier at higher frequencies. At radio frequencies there will be an additional delay since the flux density will not reach a maximum until the region starts to become optically thin as it expands down the jet. Distributed, non-uniform particle acceleration should yield a mixture of time-delayed and simultaneous flares at different frequencies.

If the jet points more closely to the line of sight than an angle Γ^{-1}, where Γ is the bulk Lorentz factor of the jet plasma, the peak of the SSC light curve is subject to a geometrical time delay corresponding to the time it takes for the flare's synchrotron photons to reach the electrons that scatter them (Sokolov et al. 2004). There should also be a tendency for the X-ray light curves to be smoother than in the optical region, since photons from millimeter to optical wavelengths will contribute roughly equally to the X-ray flux (McHardy et al. 1999). If, as discussed above, there are frequency-dependent time delays in the synchrotron light curves, these will be averaged to give X-ray light curves that have timescales characteristic of the far-infrared synchrotron emission.

One can imagine other causes of flares. For example, changes in the Doppler factor caused by acceleration or bending of the jet flow can cause nearly simultaneous variations at all wavebands, even those at somewhat optically thick frequencies (Marscher, Gear & Travis 1992). Indeed, VLBI images of jets reveal strong bending on parsec scales (e.g., Jorstad et al. 2001a, 2004; Kellermann et al. 2004), so such flares should occur at least some of the time.

3 EXPECTED CONNECTIONS BETWEEN LIGHT CURVES AND IMAGES

The most dramatic variability seen in VLBI images of relativistic jets is the appearance of superluminal knots. Even increases in the flux of the core can usually be ascribed to new knots that at first are blended at the ~ 0.1 milliarcsec resolution of mm-wave images (Savolainen et al. 2002). Rapid changes (timescales of weeks or less) in polarization often accompany the emergence of the knots down the jet, many of which have stable polarization that is different from the core or the rest of the jet (e.g., Jorstad et al. 2005).

It is very tempting—and at the heart of shock-in-jet ("internal shock") models—to associate both the superluminal knots and flux outbursts with the same episode of infusion of extra energy into the jet. If this association is correct, then major flares at high frequencies should coincide with the appearance of a superluminal knot and a corresponding radio flare. Time delays between the start and peak of a flare and the epoch when the knot is at the position of the core on the images can then inform us as to the relative position of the high-frequency emission and the mm-wave core of the jet.

4 CONNECTION BETWEEN ACTIVITY IN THE CENTRAL ENGINE AND THE JET

Combined X-ray light curves and sequences of radio images of microquasars (e.g., Mirabel & Rodríguez 1998) demonstrate that energetic events in the jet follow changes in the central engine. We have discovered similar behavior the Fanaroff-Riley class 1 (FR 1) radio galaxy 3C 120 (Marscher et al. 2002). In this object, dips in the X-ray flux and hardening of the spectrum precede the appearance of bright superluminal knots moving away from the core of the radio jet. The time delay of about 60 days indicates that the core is on the order of a parsec from the black hole. The X-ray dips are not as pronounced as in microquasars (see, e.g., Fender & Belloni 2004), so only part of the rich phenomenology of accreting stellar-mass black holes extends to their supermassive counterparts. This is expected, since the inner accretion disk of a stellar-mass black hole is hot enough to emit X-rays, while that of a supermassive black hole is not. Furthermore, the size scales increase with black-hole mass, but the propagation velocities (speeds of sound and light, Alfvén speed) do not. Processes that remain coherent over a given time interval will not affect as large a fraction of the emitting volume in the more massive case.

The author and collaborators have been monitoring the FR 2 radio galaxy 3C 111 since March 2004. At the onset, the X-ray flux was in a deep minimum from which it rose steadily over a six-month period. Three months after the minimum a very bright superluminal knot started to separate from the core of the radio jet, observed with the VLBA at 43 GHz. This dip-ejection sequence may therefore be a general characteristic of radio-loud AGN.

5 LONG-TERM, WELL-SAMPLED MULTIWAVEBAND OBSERVATIONS OF TWO BLAZARS

Figures 2 and 3 display multiwaveband light curves of two highly variable quasars that my collaborators and I have been monitoring, PKS 1510−089 ($z = 0.361$) and 3C 279 ($z = 0.538$). As expected, most X-ray flares in both sources can be associated with ejections of superluminal radio knots, as marked by vertical arrows in the figures. The apparent speeds are extremely high: $28–46c$ in PKS 1510−089 (Jorstad et al. 2005) and up to $21c$ in 3C 279 (Jorstad & Marscher 2005). The first of these papers determines the Doppler factor by comparing the timescale of variability of knots with their sizes. This allows derivation of the Lorentz factor and angle to the line of sight. A detailed kinematic model of the changing apparent speed and direction of motion allows the same in 3C 279. Jorstad et al. (2005) conclude that the jet in PKS 1510−089 has a variable Lorentz factor that reaches 48 with a Doppler factor up to 44, while the Lorentz factor in 3C 279 is as high as 24 and the Doppler factor has a value up to 40. The very high Doppler factors explain why these are such extreme blazars.
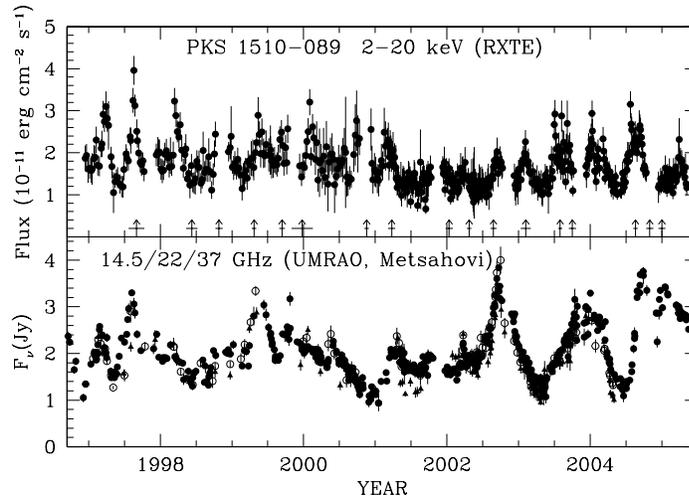
Fig. 2 X-ray and radio light curves of the quasar PKS 1510−089. Arrows give times of known ejections of superluminal radio knots up to 2005.0. Data are from Marscher et al. (2004, 2006).

There is a strong correlation between the radio and X-ray variations in PKS 1510−089 and between the optical and X-ray light curves in 3C 279 (Marscher et al. 2004). In each case, the X-rays usually lag the lower-frequency emission. The cross-correlation of the entire light curves gives a radio/X-ray lag of 6 ± 6 days in PKS 1510−089 and an optical/X-ray lag of 15 ± 15 days in 3C 279, where the standard deviation cited corresponds to the FWHM of the peak in the discrete cross-correlation function. These "reverse" time delays are consistent with the expectation of SSC models, as described above. This is perhaps the only viable explanation for PKS 1510−089, given that variations at such a low frequency (14.5 GHz) lead those at X-ray energies. In 3C 279, on the other hand, frequency stratification of the synchrotron emission could also delay the peaks of X-ray flares relative to those in the optical.

The superluminal ejections usually correspond to radio flares in the quasar PKS 1510−089, although sometimes the rising flux of the new knot is canceled out in the light curve by the decay of the previous event. The X-ray lag relative to the radio variations implies that in this quasar the X-rays come from the radio-emitting portion of the jet. Jorstad et al. (2001b) have drawn a similar conclusion regarding the γ-ray emission of blazars. This is based on a statistical association of superluminal ejections with high γ-ray flux states that lag behind the epoch when the radio knot coincided with the core.

In 3C 279 the X-ray lag relative to the optical variability implies that the X-rays come from near or downstream of the optically emitting region. The radio variations at 37 GHz are delayed by 140 ± 40
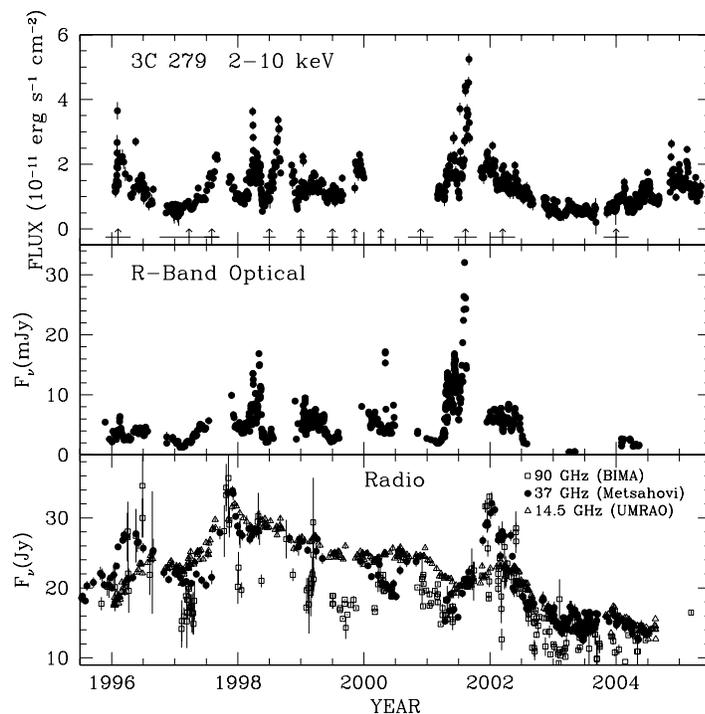
Fig. 3 X-ray, optical, and radio/mm-wave light curves of 3C 279. Arrows give times of known ejections of superluminal radio knots up to 2004.3. Ejections in mid-1996 may have been missed because of gaps in the time coverage of VLBA observations. Data are from Marscher et al. (2004, 2006).

days relative to the X-ray light curve. This is similar to the typical time from the start to the peak of radio outbursts in this quasar at high radio frequencies (Langfors et al. 2006). This behavior agrees qualitatively with the expectations of the shock-in-jet model, as discussed above.

The power spectral density of the X-ray and radio flux variations of these two objects indicate that the observed fluctuations correspond to "red noise," i.e., there are no significant features suggesting periodicities in the light curves.

There are many more multiwaveband observations of blazars than can be discussed here. None of these have the many-year closely-sampled light curves extending from radio to X-ray frequencies that characterize our study of PKS 1510−089 and 3C 279.

6 THE COMPLEX CASE OF THE QUASAR 3C 273

The quasar 3C 273 ($z = 0.158$) is a blazar at radio to IR wavelengths, but in the optical and uv, the big blue bump usually dominates. According to Grandi & Palumbo (2004), the X-ray emission above 2 keV is a mixture of two components: a Seyfert-like spectrum with typical energy spectral index of 0.8 and nonthermal emission from the jet with a spectral index of 0.52±0.05. Figure 3 displays X-ray light curves in medium (2–10 keV) and hard (10–200 keV) X-ray bands from RXTE observations by the author and collaborators. Despite smoothing of the hard X-ray light curve, many of the peaks and valleys are more sharply defined than in the medium-energy band. This suggests that the jet emission is highly variable, since the flatter spectrum of the jet implies that the harder X-rays are more sensitive to variations in its flux.

On the other hand, archival light curves at wavelengths of 3 and 1.3 mm are not correlated with those at the X-ray bands. The main cross-waveband correlation in the past has occurred between the X-ray and near-IR K band on timescales of days (McHardy et al. 1999). The author and S. Jorstad will observe 3C 273
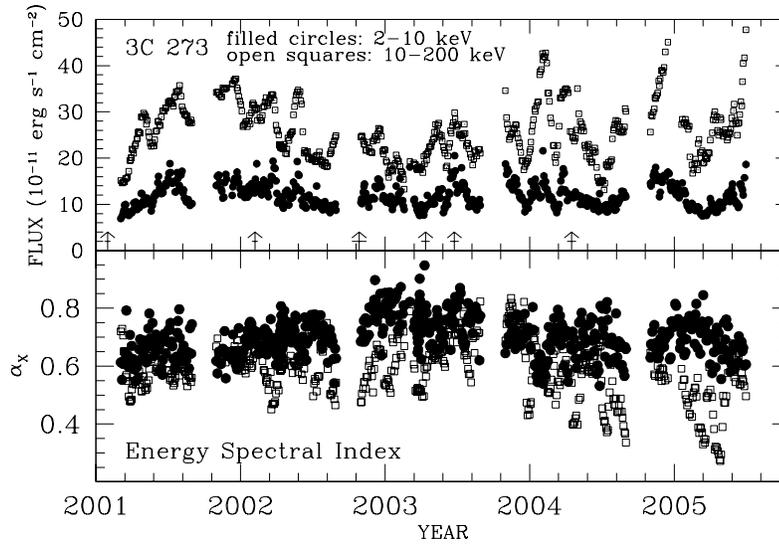
Fig. 4 X-ray light curve and spectral index vs. time at two energy bands, from the RXTE PCA (2–10 keV) and HEXTE (10–200 keV) instruments. In order to improve the signal-to-noise ratio, the HEXTE data have been median-smoothed with a smoothing time of ± 10 days. Error bars are smaller than the data points for the fluxes. Errors are not shown for the spectral indices; they are typically ± 0.1. Arrows give times of known ejections of superluminal radio knots up to 2005.0. Data are from Marscher et al. (2004, 2006).

with the *Spitzer* Space Telescope at mid- and far-IR bands over a 35-day period in order to determine how well correlated the emission is on somewhat longer timescales.

7 FUTURE OBSERVATIONAL PROGRAMS

Mounting campaigns to gather well-sampled multiwaveband light curves of many blazars is a daunting task. At many wavebands (e.g., IR and 0.3–3 mm) the telescopes were built primarily for other purposes, yet proper blazar monitoring requires telescope time on a frequent, regular basis. Fortunately, the γ-ray missions GLAST and, to a lesser extent, AGILE will provide excellent time sampling of tens of blazars that are bright γ-ray sources. We need to support these instruments with ample ground-based observations. This is being organized at optical wavelengths. But we need to lobby for financial support for—as well as telescope time on—X-ray, IR, submm- and mm-wave, and radio telescopes, including the VLBA. Our observations should include polarization whenever possible, since a superluminal knot emitting at optical wavelengths can potentially be identified on VLBI images through its polarization position angle. In addition, strong frequency dependence of polarization (higher polarization at higher frequencies) is a key signature of frequency stratification of synchrotron radiation.

8 CONCLUSIONS

Our multiwaveband monitoring including RXTE X-ray observations illustrates the diversity of different subclasses of radio-loud AGN. In blazars, the emission is from highly beamed relativistic jets in which the emission at different wavebands is only partially co-spatial. In radio galaxies and quasars with unbeamed optical emission, the spectrum from radio to IR wavelengths is dominated by synchrotron radiation, while in X-rays the central engine plays a major role. The most perplexing case is 3C 273, in which the hard X-ray emission is apparently from the jet but is not correlated with the light curves at millimeter wavelengths. This suggests greater frequency stratification of the jet than in the more extreme blazars. Perhaps in the latter we only see the jet from the mm-wave core outward, while in 3C 273 we can also see the section between the central engine and the core (see Fig. 1). If this is the case, analysis of more comprehensive multiwaveband

light curves of 3C 273 might reveal the physical processes responsible for the acceleration and collimation of the jet.

It is clear from observations of microquasars and the radio galaxies 3C 120 and 3C 111 that events affecting the X-ray emission from the central engine modulate the energy flow into the jet. Exactly what takes place in these events is controversial (see Fender & Belloni 2004). As discussed above, only some of the processes that affect the X-ray emission scale up with the mass of the black hole, while others seem to weaken as the volume of the central engine increases and the temperature of the inner accretion disk decreases with mass.

Unfortunately, RXTE is getting on in years and will unlikely be in operation much longer before another detector dies or the funding is cut off. A new X-ray timing telescope is sorely needed, preferably one that can observe a large fraction of the sky simultaneously with high sensitivity. Perhaps even more urgent are advances in theoretical understanding that can come from better modeling of the accretion disk, corona, and jet of an AGN.

References

Fender, R., Belloni, T. 2004, ARA&A, 42, 317

Grandi, P., Palumbo, G.G.C. 2004, Science, 306, 998

Jorstad, S. G., et al. 2001a, ApJS, 134, 181

Jorstad, S.G., et al. 2001b, ApJ, 556, 738

Jorstad, S.G., et al. 2004, AJ, 127, 3115

Jorstad, S.G., et al. 2005, AJ, 130, in press

Jorstad, S.G., Marscher, A.P. 2005, Mem. S.A.It., 76, 106

Kellermann, K.I., et al. 2004, ApJ, 609, 539

Langfors, E., et al. 2006, A&A, submitted

Lister, M.L., Marscher, A.P. 1997, ApJ, 476, 572

Marscher, A.P. 2005, Mem. S.A.It., 76, 13

Marscher, A.P., et al. 2002, Nature, 417, 625

Marscher, A.P. et al. 2004, in X-Ray Timing 2003: Rossi and Beyond, ed. P. Kaaret, F.K. Lamb, & J.H. Swank (Melville, NY: AIP), 167

Marscher, A.P., et al. 2006, in preparation

Marscher, A.P., Gear, W.K. 1985, ApJ, 298, 114

Marscher, A.P., Gear, W.K., & Travis, J.P. 1992, in Variability of Blazars, ed. E. Valtaoja M. Valtonen, Cambridge U. Press, 85

McHardy, I.M., et al. 1999, MNRAS, 310, 571

Meier, D. L., Koide, S., & Uchida, Y. 2000, Science, 291, 84

Mirabel, I.F., Rodr´ıguez, L.F. 1998, Nature, 392, 673

Savolainen, T., Wiik, K., Valtaoja, E., Jorstad, S.G., Marscher, A.P. 2002, A&A, 394, 851

Sokolov, A., Marscher, A. P., & McHardy, I. M. 2004, ApJ, 613, 725 ApJ, 605, 656